Freezing Range, Melt Quality, and Hot Tearing in Al-Si Alloys

MUHAMMET ULUDAĞ, REMZI ÇETIN, and DERYA DISPINAR

In this study, three different aluminum-silicon alloys (A356, A413, and A380) that have different solidification morphology and solidification ranges were examined with an aim to evaluate the hot tearing susceptibility. T-shape mold and Constrained Rod Casting (CRC) mold were used for the characterization. Reduced Pressure Test (RPT) was used to quantify the casting quality by measuring bifilm index. It was found that bifilm index and solidification range have an important role on the hot tearing formation. As it is known, bifilms can cause porosity and in this case, it was shown that porosity formed by bifilms decreased hot tearing tendency. As the freezing range of alloy increases, bifilms find the time to unravel that reduces hot tearing. However, for eutectic alloy (A413), due to zero freezing range, regardless of bifilm content, hot tearing was never observed. A380.1 alloy had the highest tendency for hot tearing due to having the highest freezing range among the alloys investigated in this work.

https://doi.org/10.1007/s11661-018-4512-8

I. INTRODUCTION

HOT tearing is one of the most important defects in aluminum alloys. It has been reported that the main reasons that cause hot tearing are the contraction in mushy zone, restricted shrinkage, and lack of feeding.[1,2] It is not easy to estimate this defect because of some complex events occurring simultaneously during solidification. Although there are several studies on hot tearing,[3–8] yet, it cannot be fully explained.[1] The "uncertainty" in the characteristic properties of hot tearing has been listed as follows:

- Occurs as messy in the form of branched cracks.
- Main tearing and its extensions are observed to be intergranular.
- Defect surface has a dendritic morphology.
- Defect surface is usually packed with heavy oxides.
- Generally located on hot spots where shrinkage takes place.
- Not always seen under the same conditions.
- Specific to certain alloys; not seen in all alloys.

Campbell[9] recommend that this problem can be controlled by

- Chill applications
- Grain refinement
- Working with different alloys
- Using suitable mold design
- Proper runner and sprue design (controlled filling)

Eskin *et al.*[10] have extensively studied the characterisation of hot tearing phenomena and claimed that the stage of separation between dendrites is crucial and sensitive for the alloys that have a wide solidification range. Hot tearing formation was divided into four levels as described below:

i. Mass feeding where liquid and solid act freely.
ii. Interdendritic feeding where remaining liquid has to pass dendritic network. Network permeability is still very large to prevent pore formation.
iii. Interdendritic separation: as solid fraction is increased, liquid is trapped in interstitial spaces or immobilized because of surface tension. At this level, shrinkage occurs where solid network permeability decreases and material shrinks.
iv. Solid feeding where only the liquid pockets remain and the cast part has a significant strength on the last level of solidification ($f_s > 0.9$). Hot tearing can occur at this level.

Eskin *et al.*[10] focused on the last two levels because interdendritic separation is quite sensitive to hot tearing in alloys that have a large solidification range.

A study that measures hot tear length using a "U" shape mold was used to investigate the effect of silicon ratio on hot tearing in Al-Si alloys.[11] It was found that silicon can start to initiate hot tearing until 1.9 wt pct Si. However, the hot tearing can be decreased by silicon

MUHAMMET ULUDAĞ is with the Metallurgical and Materials Engineering Department, Bursa Technical University, Bursa, Turkey; Contact e-mail: dr.uludagm@gmail.com REMZI ÇETIN is with the Materials Engineering Department, KTO Karatay University, Konya, Turkey. DERYA DISPINAR is with the Metallurgical and Materials Engineering Dept., Istanbul University, Istanbul, Turkey.
Manuscript submitted August 7, 2017.
Article published online February 15, 2018

additions after 1.9 wt pct. Pumphrey[12] studied hot tearing using six different alloys: Al-Si, Al-Cu, Al-Mg, Al-Fe, Al-Mn, and Al-Zn. The alloys were prepared by high-purity aluminum and high-purity master alloys. It was found that at low additions, hot tearing is high; and at high additions, hot tearing is low. And it was claimed that chemical composition of alloys and overheating affect both grain structure and hot tearing. In Al-Si, Al-Mg, Al-Cu, and Al-Zn alloys, the hot tearing can be decreased by columnar-to-equiaxed transition with increased overheating.[12,13]

Verö[11] investigated the effect of eutectic ratio on the hot tearing and it was found that hot tearing tendency can increase at low eutectic ratios. However, hot tearing is decreased substantially at high eutectic ratios. Copper content in an alloy has an effect on hot tearing. The copper content up to 7 wt pct is reported to be dangerous for hot tearing but above this value, hot tearing tendency starts to decrease.[7]

Pokorny *et al.*[14] investigated hot tearing in AZ91D alloy by using T-shape mold. The contraction of the horizontal bar is restrained during solidification, and hot tearing occurs at the junction between the horizontal bar and the vertical sprue. The study on the effect of mold temperatures from 140 °C to 380 °C showed that the mold temperature has an important effect on hot tearing susceptibility. The simulation results suggest that the predicted damage is in agreement with the hot tears observed in the experimental castings, both in terms of location and severity. Thus, there was a good correlation between experimental work and simulation. Bichler *et al.*[15] found the same effect on hot tearing of AZ91D and AE42 magnesium alloys.

Bichler and Ravindran[16] used T-shape mold for the hot tearing sensitivity of magnesium alloys. A numerical model was proposed to define hot tearing. It was claimed that hot tearing index reached a maximum at a casting location coincident with the region of hot tearing. However, the path of hot tear propagation could not be identified using the numerical model. It was also claimed that nucleation of microcracks occurs at a stress concentration that is on the 90 deg corner of the junction of the horizontal bar and the downsprue.

Nasr Esfahani and Niroumand[17] carried out a study on the effect of casting temperature on hot tearing of A206 aluminum alloy using instrumented constrained T-shaped casting method. Casting apparatus was designed to measure contraction load in the casting during solidification. It was found that hot tearing susceptibility increases with increased casting temperature. This was associated with reduced cooling rate, increased solute segregation, and more localized hot spot formation at the T-junction area. It was claimed that grain size had affected the initiation of hot tears that was increased with increasing casting temperature.

D'Elia *et al.*[18] also studied with T-shape mold to investigate hot tearing formation in B206 aluminum alloy. It was found that titanum-boron grain refiner additions resulted in a significant decrease in grain size and a transformation from dendritic to globular morphology. These globular grains were less prone to the formation of hot tears and thus, the grain-refined alloys displayed significantly less susceptibility to hot tearing. It was claimed that grain size, microstructural features, and strain distributions at the junction between the horizontal casting bar and the downsprue have an important effect on the hot tearing formation.

Cao and Kou[19] studied hot tearing in ternary Mg-Al-Ca alloys by using CRC mold. To explain how hot tearing occurs in these alloys, the secondary phases, eutectic content, solidification path, and freezing range were examined. It was found that the alloys that have the widest freezing range and the lowest eutectic content are the most susceptible to hot tearing, while the alloys that have opposite features are less susceptible to hot tearing.

Lin *et al.*[20] carried out a study on hot tearing of wrought aluminum alloys (AA1050, AA5182, and AA3104) by using CRC mold. Mechanisms of hot tearing were investigated *via* microstructural examination of hot tears. Hot tearing in AA1050 and AA5182 alloys was characterized as interdendritic separation during solidification. The results of this study showed that hot tearing susceptibility (HTS) ranking of the alloys was not explained by non-equilibrium freezing range. It was claimed that hot tearing sensitivity is related to the average grain size of the castings. If the grains size of a casting is above 200 μm, HTS of the casting will be sensitive to grain refining. The most effective factor in reducing HTS in AA5182 alloy was related to the grain refining.

Pekguleryuz *et al.*[21] studied on developing castability index for magnesium die casting alloys using CRC mold. A castability index was proposed based on alloy characteristics such as solid thermal conductivity, non-equilibrium freezing range, and hot tear sensitivity. Hot tear sensitivity of AJ alloys has been determined and compared to other commercial magnesium die casting alloys. It was found that AZ91D alloy has the lowest hot tear sensitivity of 20 followed by AJ52 at 24, which closely approximates to AZ91D. It was claimed that hot tear and its rating (HTS) was able to predict the trend in diecastability of magnesium alloys.

Pekguleryuz *et al.*[13] also studied on hot tear susceptibility of aluminum-silicon binary alloys. CRC mold was used in the study. It was found that increasing silicon content has the ability to decrease the hot tear susceptibility. Solidification shrinkage, non-equilibrium freezing range, dendrite arm spacing, and grain size affect hot tear severity directly. It was also found that Al-0.5 pct Si alloy that has the largest non-equilibrium freezing range, the highest solidification shrinkage, the largest dendrite arm spacing, the lowest amount of eutectic phases and, hence, had the highest HTS.

Kamguo Kamga *et al.*[22] studied hot tearing of aluminum-copper B206 alloys with iron and silicon additions using CRC mold to examine the combined effect of these additions on hot tear resistance. It was found that hot tearing formation was increased gradually with iron content. This was attributed to the conditions that led to the formation of the β(FeCu) phases while silicon had an opposite effect. The hot tearing sensitivity of the alloys was characterized with a new index that shows a very good correlation with the

Table I. Chemical Composition (in Wt Pct) of the Alloys Used in the Study

Alloys	Si	Fe	Cu	Mn	Mg	Zn	Ti	Al
A356	6.80	0.19	0.003	0.001	0.30	0.011	0.108	rem.
A413	11.77	0.19	0.006	0.001	0.005	0.016	0.006	rem.
A380.1	8.14	0.64	3.12	0.44	0.22	0.49	0.02	rem.

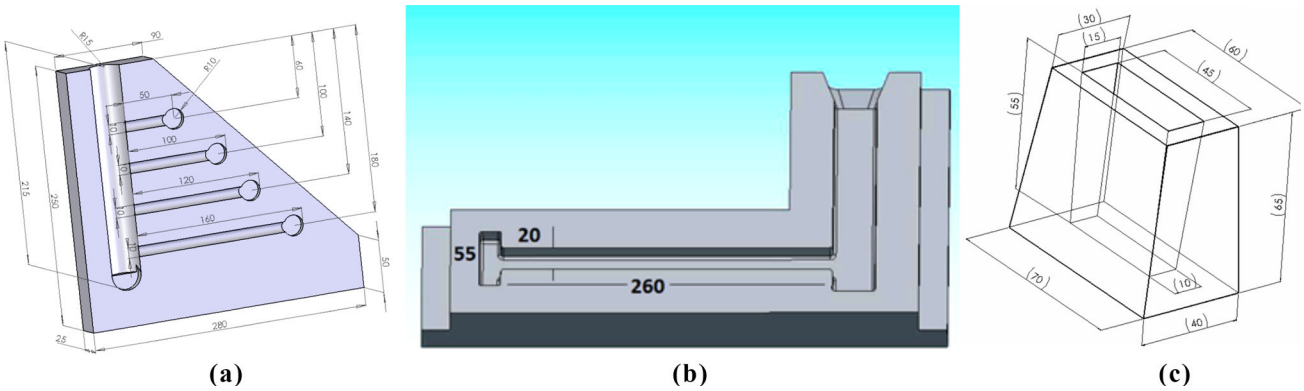

Fig. 1—Dimensions of the molds used in the study. (*a*) CRC, (*b*) T, (*c*) RPT mold.

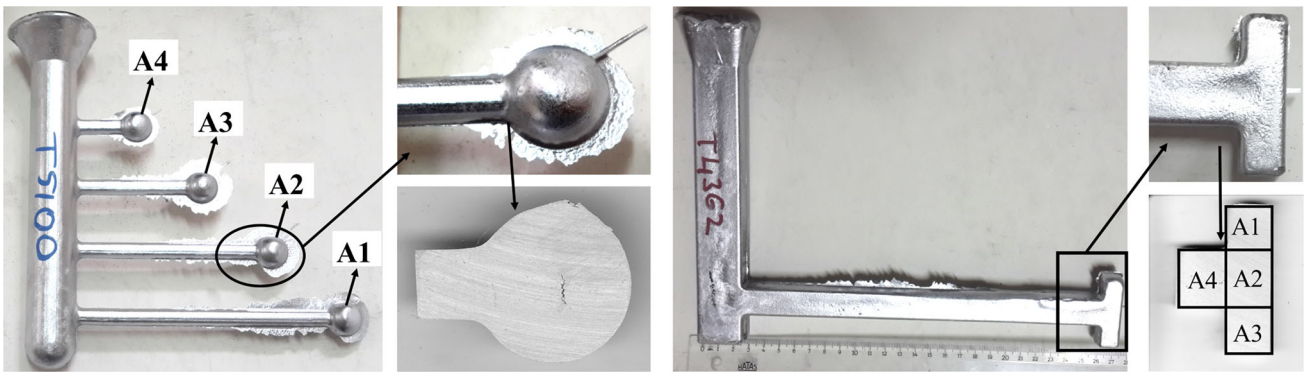

Fig. 2—Cast parts and sample locations for pore analysis.

Katgerman's[23] hot tearing index (HCS). In this index, the temperature where inadequate feeding started had to be determined.

Li *et al.*[24] studied the characterization of hot tearing in Al cast alloys by using an instrument which allows measuring the contraction force/displacement and temperature during solidification. It was claimed that the test results were repeatable and reliable. Hot tearing was alloy dependent. A356 alloy has high resistance to hot tearing, while M206 has the tendency to tear under the same conditions. Interdendritic cracking was evident in M206. Filled cracks were seen around the transition area. The flow of interdendritic liquid plays an important role in filling the incipient cracks. It was found that at 561 °C and at fraction solid of 0.89, solid network starts in A356 alloy while it starts at 601 °C and at fraction solid of 0.80 in M206 alloy. Also, Li *et al.*[25,26] reported another study where the severity of hot tearing and linear contraction was found to decrease significantly when mold temperature was increased. Increasing pouring temperature resulted in more severe hot tearing. On the other hand, grain refinement can decrease hot tearing in alloy 206 significantly and hot tearing can be eliminated if the alloy has a fine globular microstructure.

On the other hand, there are several studies that evaluate hot tearing formation by using various criteria. Some of those studies focused on the effect of stress,[27–33] some focused on strain[9,31,34,35] and others used strain rate.[6,36,37] Most famous ones are the studies of Clyne and Davies,[38] Feurer,[39] and Katgerman[23] on extracting a criterion for hot tearing. The aim of these criteria is based on estimating hot tearing tendency in alloys prior to casting. The common feature of these criteria is the ''circa'' estimation because there was never a perfect correlation between the estimators and experimental findings. However, they were still good enough to explain hot tearing formation.

Bifilms are the casting defects that are formed due to the entrainment of the surface oxide film into the liquid aluminum.[1] The folded oxide surfaces have zero bonding and air gap in between them. Thus, it acts as a crack in the liquid. During solidification, they may unravel and open up

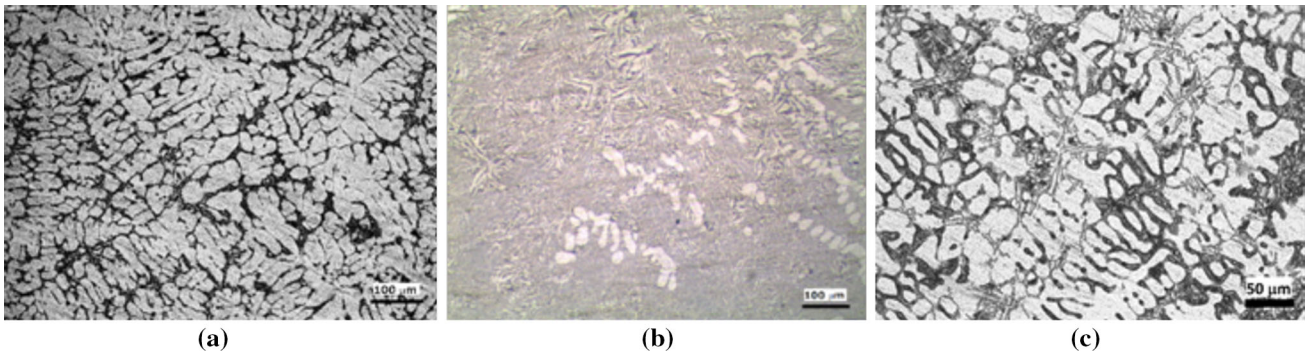

Fig. 3—Microstructure images of the alloys. (*a*) 356, (*b*) 413, (*c*) 380.

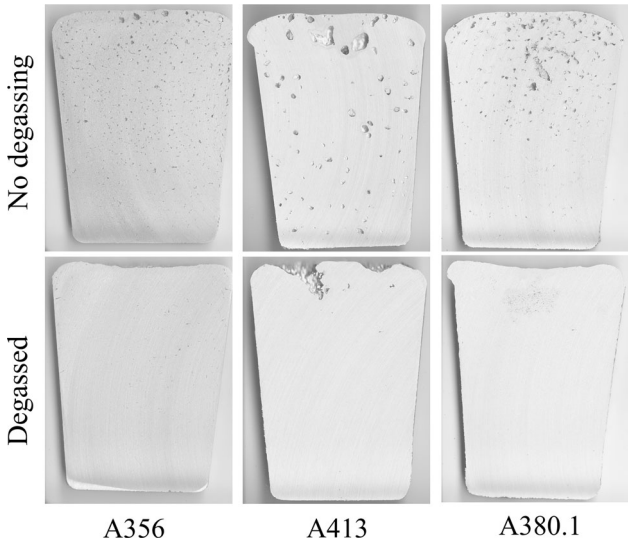

Fig. 4—Cross section of RPT samples before and after degassing.

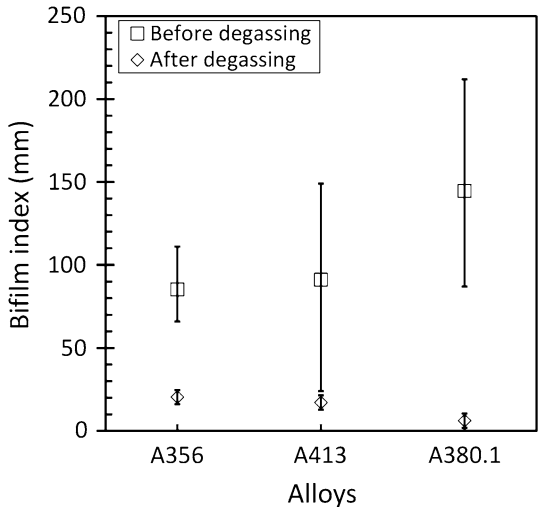

Fig. 5—Qualities (bifilm index) of the castings before and after degassing.

to cause porosity.[40] This process of unraveling depends on the size, shape, and type of the oxide. Therefore, existing of bifilms in the solidified cast part will lead to deterioration of many properties. There are several works in the literature[10,41–44] that characterize these findings, many of which show the decrease in mechanical properties. Dispinar[45–50] has worked on the quantification of bifilms (*i.e.*, melt cleanliness) and proposed an index called bifilm index. This index is measured by Reduced Pressure Test (RPT). A sample is solidified under 100 mbar vacuum to enhance the unraveling of bifilms and the cross section of the sample is subjected to image analysis to measure the number and size of porosity. The sum of the maximum length of pores is calculated to give a numerical indication of melt quality. Since all pores are initiated by bifilms, consequently, the higher the bifilm index would mean lower the melt cleanliness.

When all the literature work on hot tearing is investigated, it can be seen that there are three characteristics of this defect:

i hot tearing does not occur under all casting conditions,
ii hot tearing is not seen in all alloys,
iii hot tearing occurs randomly and indiscriminately

These definitions cannot explain hot tearing formation completely. Yet, this is the reason why the term "circa" was used above, because the approximations and analytical approaches do not 100 pct justify experimental findings. Regarding these uncertainties in the list above, a new approach was proposed which consisted of a new index that contained liquid metal cleanliness that was never considered before. Thus, three different alloys with different freezing ranges were investigated in order to characterize the hot tearing tendency.

II. EXPERIMENTAL DETAILS

Three different alloys that have different solidification ranges were used in this study. A356 and A413 alloys were provided from Eti Aluminyum, Turkey and A380.1 alloy was provided by Cevher Döküm, Turkey. The chemical compositions of these alloys are given in Table I.

Hot tearing test was carried out using two different die molds: CRC and T shape. Reduced pressure test (RPT) was used to quantify casting quality.[51] The dimension of the hot tearing molds and RPT mold is given in Figure 1.

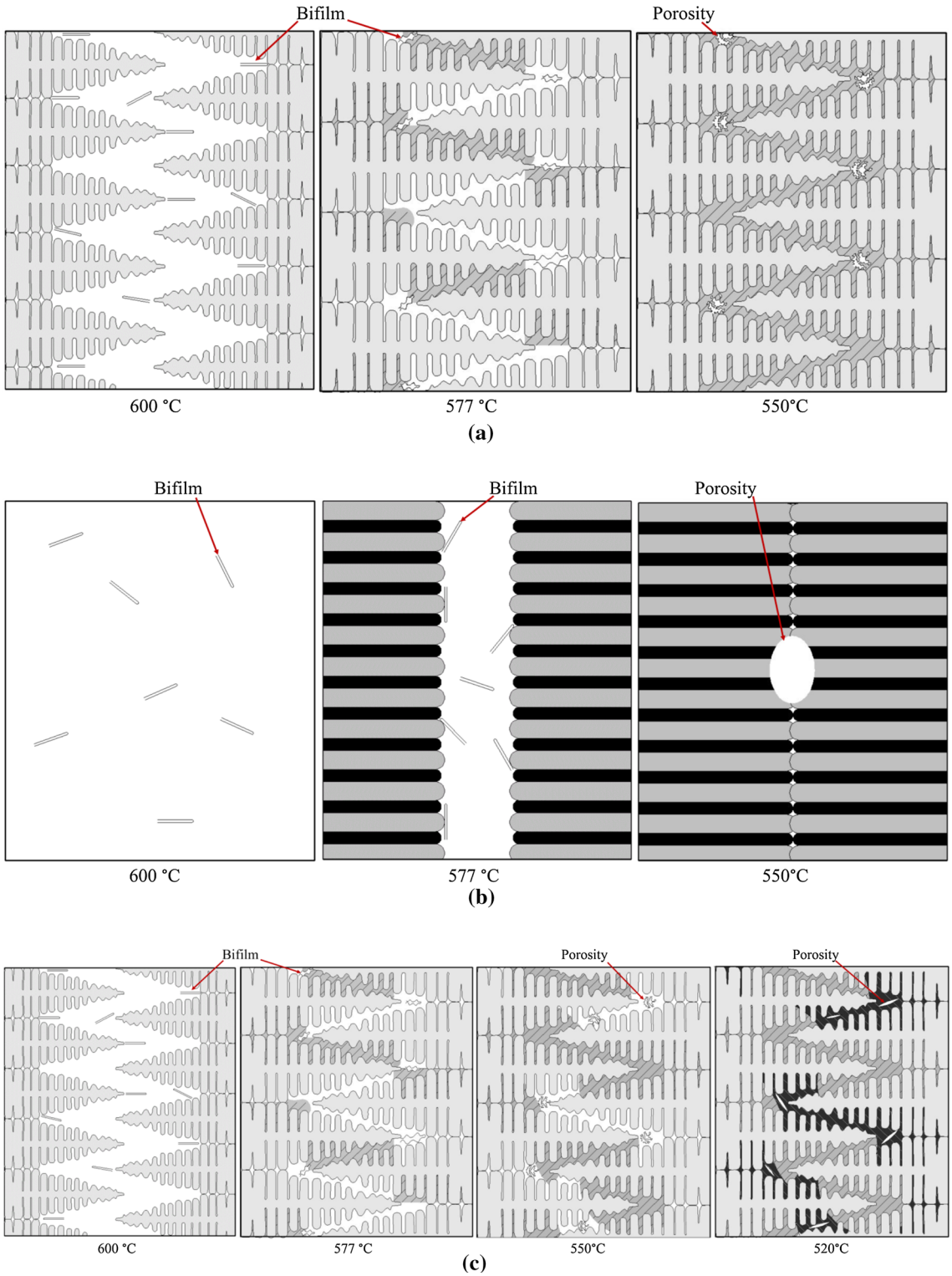

Fig. 6—Pore formation mechanism in the presence of bifilms with regard to the solidification mode. (*a*) A356: light gray: dendrites, dashed: Al-Si eutectic. (*b*) A413: Al and Si phases (eutectic). (*c*) A380.1: light gray: dendrites, dashed: Al-Si eutectic, black: $CuAl_2$ eutectic.

All alloys were melted in coated SiC crucible by using an electrical furnace. Casting temperatures of A356 and A380.1 alloys were 740 °C, and A413 alloy was poured at 670 °C. RPT samples were collected before pouring alloys into hot tearing molds. Castings were carried out three times under two conditions: before and after degassing. Degassing was carried out for 20 minutes with Ar by a graphite nozzle. Casting quality was calculated by means of bifilm index from RPT samples. An image analysis software (SigmaScan) was used for

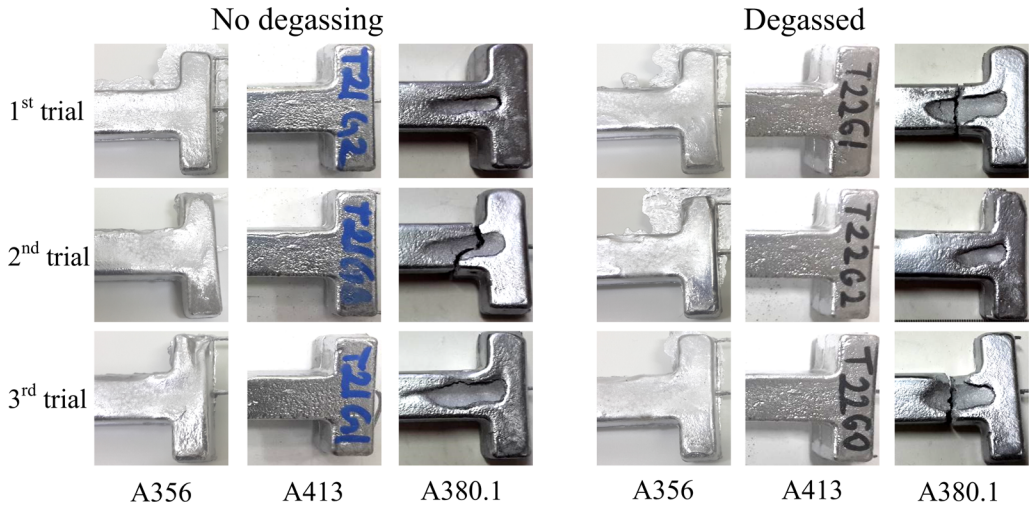

Fig. 7—T zones of the T-shape castings.

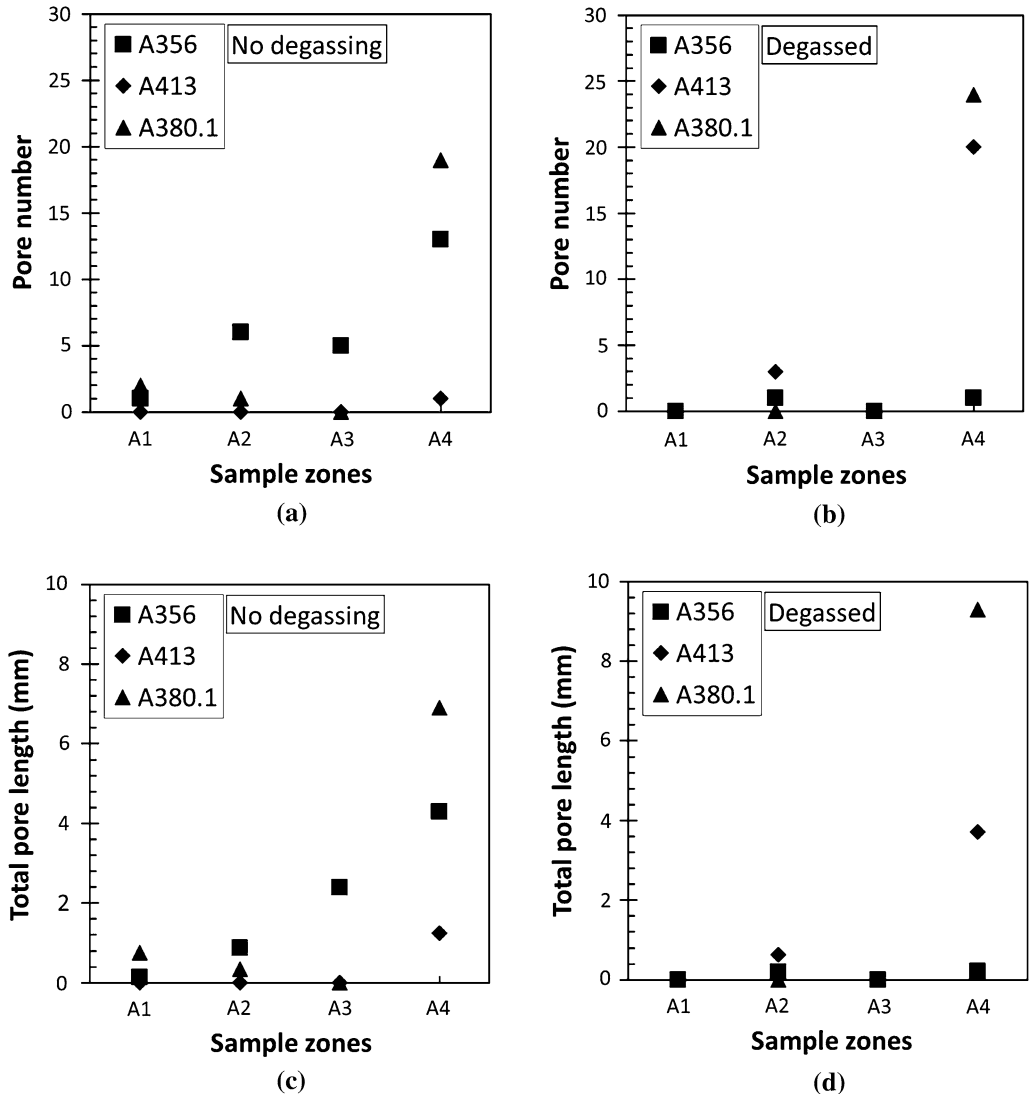

Fig. 8—(*a*) Pore numbers from T zones for no degassing condition, (*b*) pore numbers from T zones for degassed condition, (*c*) total pore lengths from T zones for no degassing condition, and (*d*) total pore lengths from T zones for degassed condition.

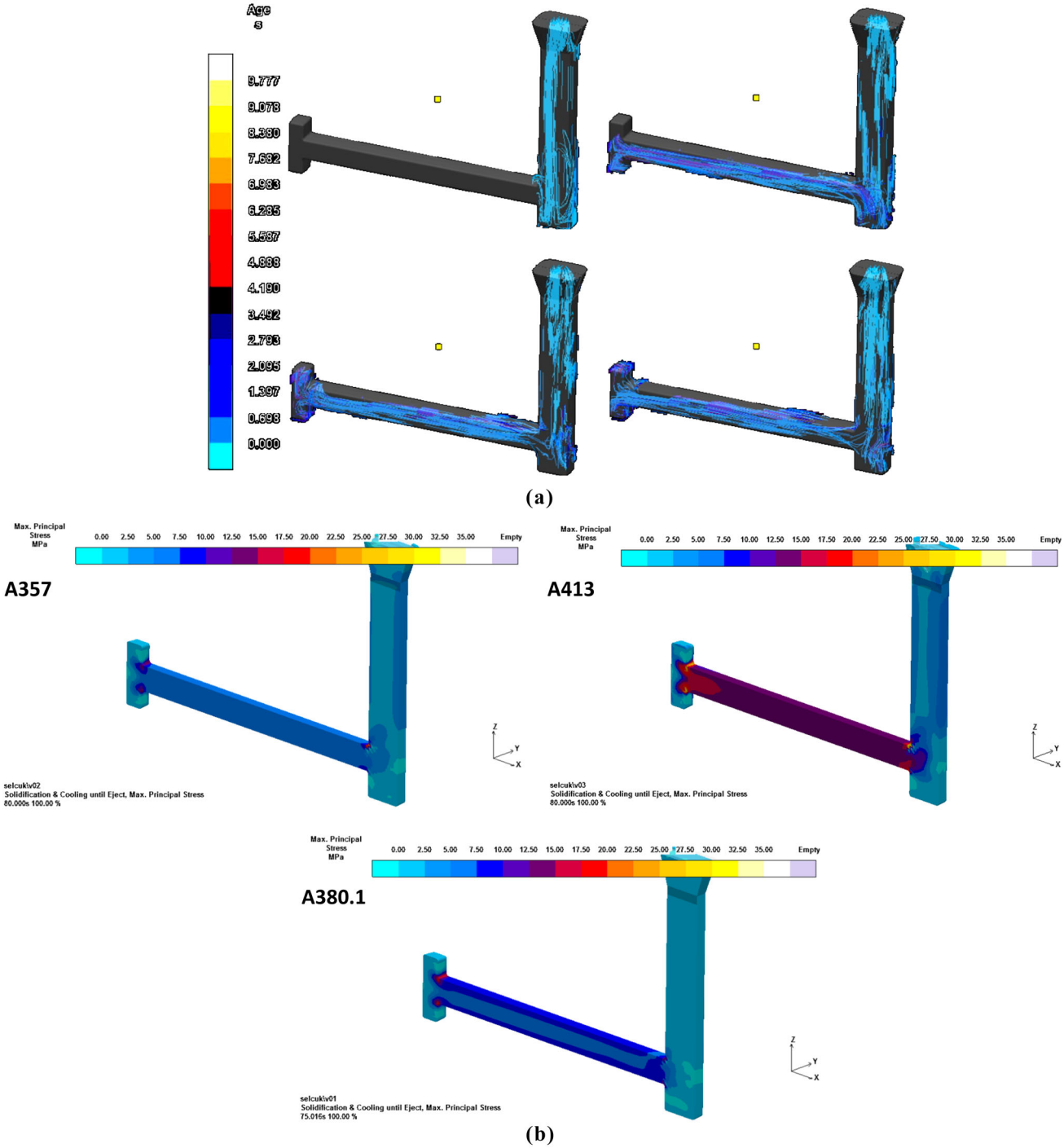

Fig. 9—(*a*) Magmasoft mold filling results showing the turbulence in A2 and A4 region. (*b*) Magmasoft stress results of three alloys.

quantification of pore size, shape and dimension. MagmaSoft was used to examine the stress and strain during the solidification of the alloys.

Pore number and total pore length were calculated for T mold and spherical zone of CRC mold as shown in Figure 2. Areas of pore calculations were marked as A1, A2, A3, and A4 on T zone. For CRC mold, areas of pore calculations were called as A1, A2, A3, and A4 from bottom to top as shown in Figure 2.

III. RESULTS AND DISCUSSION

A356 alloy has dendritic and eutectic microstructure. In this alloy, α-(Al) is solidified first and α-(Al) + Si eutectic forms second. α-(Al) dendrites can be columnar and eutectic is formed between the dendrite arms. For A413, Al + Si eutectic morphology is the only phase since the composition is at 12 Si wt pct which is the eutectic composition. This eutectic phase transformation occurs

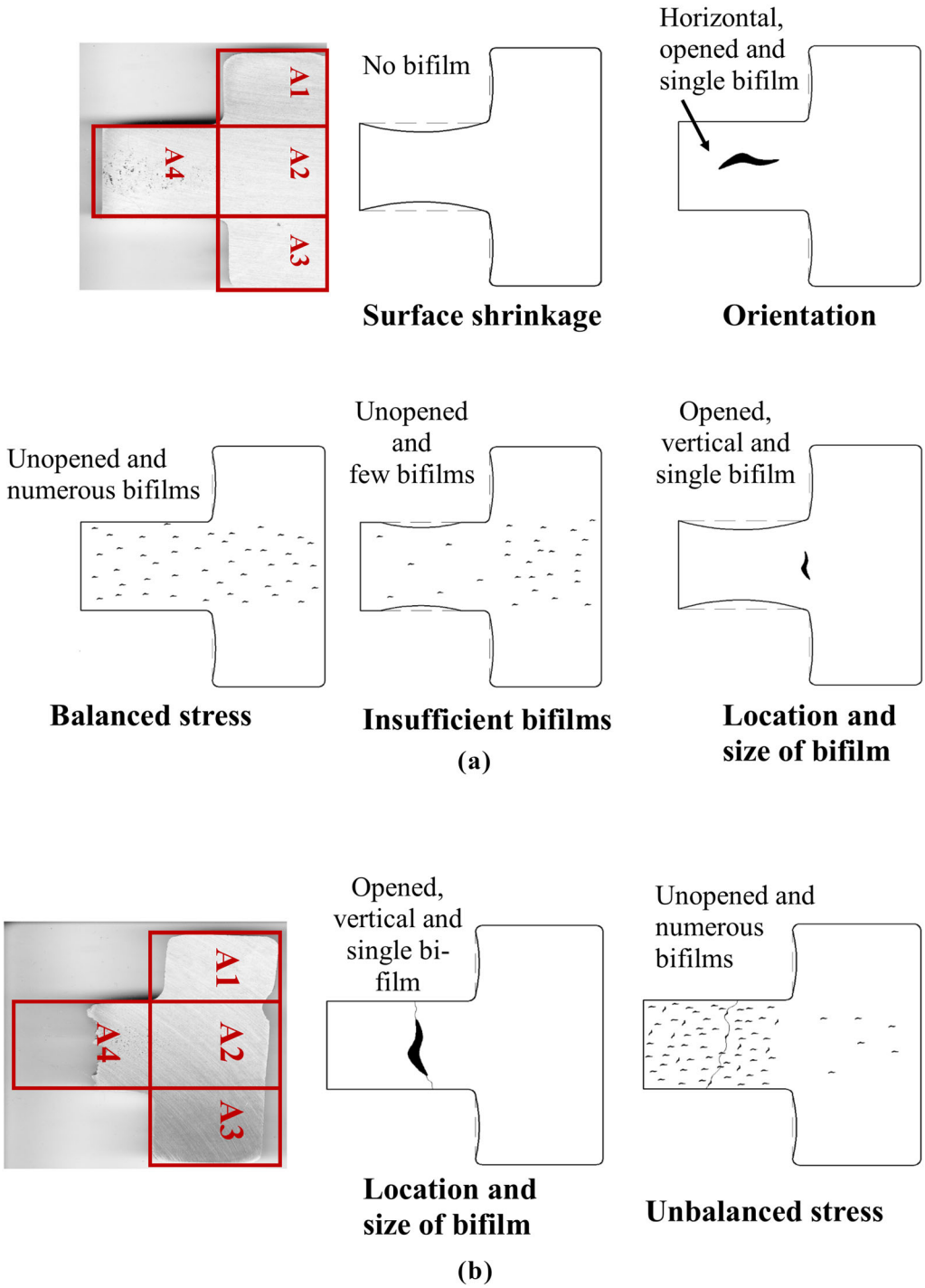

Fig. 10—Schematic images for bifilm formation (*a*) for no hot tearing, (*b*) for hot tearing.

at a single temperature where two solids phases are formed simultaneously. The feedability is more favorable in A413 alloy than A356 alloy. On the other hand, A380.1 alloy also has 8 wt pct Si and 3 wt pct Cu. The microstructural transition occurs as follows: α-(Al) dendrite, α-(Al) + Si eutectic, and α-(Al) + Cu + Si eutectic. Therefore, during the solidification process, after Al-Si eutectic phase, there stills remains a liquid phase that transforms to Al-Cu eutectic. The microstructures of the alloys used in the study are given in Figure 3. Differences among the microstructures can be easily seen on these images. As seen in Figure 3(a), A356 consists of dendrites and eutectic phase. In Figure 3(b), the microstructure of A413 consists of Al-Si eutectic and dendrites due to the change in the undercooling conditions in the presence of grain refiners. In Figure 3(b), the three phases aforementioned can be easily seen. These are the typical morphologies for those alloys.

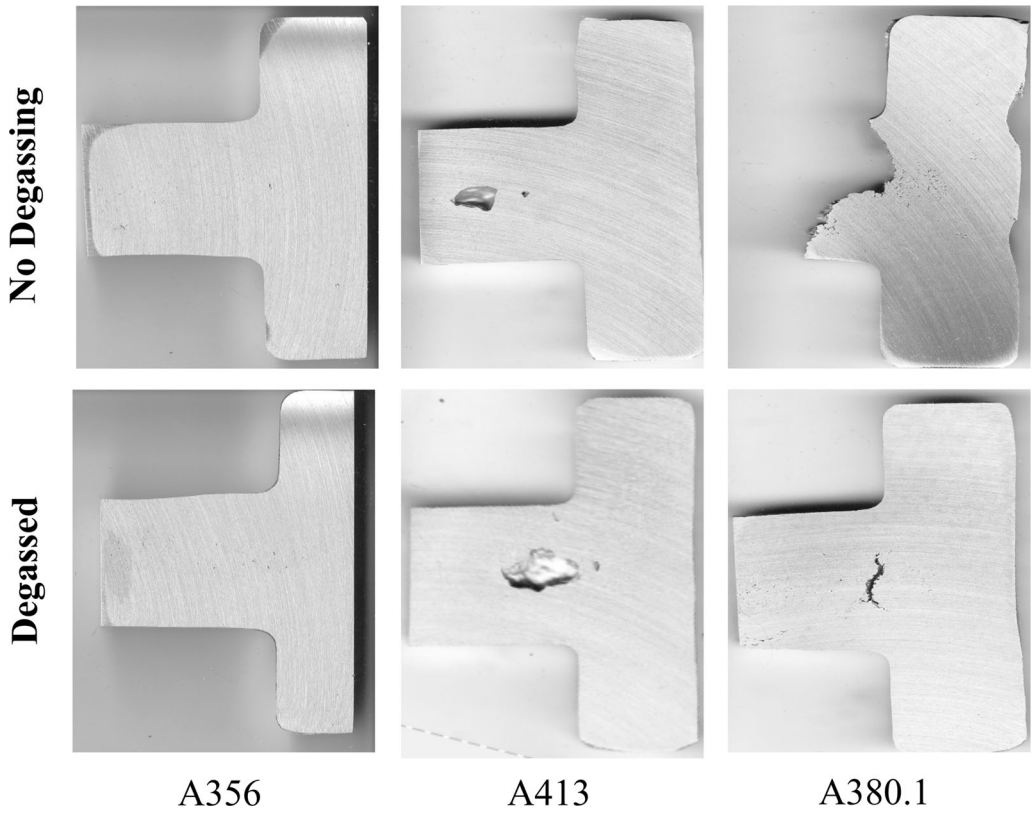

Fig. 11—A1-A4 region cross section that show bifilms and pores.

Bifilms determine the quality of casting parts.[1,40,45,46,49] It was known that bifilms can be determined by using reduced pressure test.[45,46,51] This test can help bifilms to enlarge 10 times due to 100 mbar vacuum during solidification. These can be visually examined when cross sections of RPT samples are considered. Representative images of RPT samples before and after degassing are shown in Figure 4. As can be seen, all of the three alloys have a certain amount of bifilms before degassing. Consequently, after degassing, bifilms were significantly removed from the melt.

Bifilm index values were calculated from RPT images to determine casting quality and the results are given in Figure 5. Bifilm index[51] is the sum of the total length of pores on the cross section of the reduced pressure test samples. The differences between melt conditions can be easily seen. These differences show that the degassing process was very effective. Scatter of bifilm index in the melt before degassing is an indication of how the melt is contaminated with various sizes of bifilms.[52–61] It can be seen that the worst quality melt was A380.1 with a bifilm index of 150 mm. However, after degassing, the lowest bifilm index value (*i.e.*, highest-quality melt) was also obtained in the same alloy which was 5 mm. A356 and A413 alloys have almost the same bifilm index value (20 mm) for both melt conditions.

It is important to note that each alloy has different pore morphology due the different characteristics of solidification which is mainly based on the behavior of bifilms. While there are small and numerous bifilms in A356, there are bigger and outnumbered bifilms in A413 alloy. On the other hand, A380.1 alloy has bifilms that are larger than A356 but smaller than A413. Additionally, bifilm number of A380.1 is between A356 and A413. Bifilms are surface oxides that are folded and submerged into the melt mainly due to turbulence. As Campbell[1] has shown, the microstructural changes during solidification determine whether the bifilms can unravel or not. Faster and rapid solidification hinders the growth and unraveling of bifilms. Slower cooling and the growth of large dendrites can easily push the bifilms to become unraveled. Therefore, in A356, after the formation of α-Al, the only way bifilm can open is right before the eutectic phase formation. Once the remaining liquid between the dendrites is transformed into eutectic (rapid solidification), there will no longer be pore formation. As seen in Figure 4, this is why there is numerous number of pores in A356 that is distributed along the cross section. A similar scenario applies to A380.1. On the other hand, with the same mechanism, since there is only a eutectic phase in A413, as long as bifilms open up before the liquid–solid transformation occurs, they can be observed as pores. This mechanism is schematically shown in Figure 6 for three different solidification modes.

The hot tearing formation was examined first by using T-shape mold. T zone of the T-shape mold has a hot spot. Images of T zones for all castings are given in

Fig. 12—Casting parts from CRC mold (*a*) 356, (*b*) 413, (*c*) 380.1.

Figure 7. It can be seen that A380.1 alloy is the only one that has hot tearing for both melt conditions. All cast parts of this alloy have either hot tearing or crack in all conditions. A surface sink can be seen in the cast part with crack or tear. Campbell[1,62] had shown that in the absence of bifilms, liquid/solid contraction stresses are so strong that it can lead to surface sink. On the other hand, A356 alloy does not have any hot tearing formation but has a surface sink in all conditions. However, A413 alloy has neither hot tearing nor surface sink. There are two different features to separate these three alloys from each other. One is solidification morphology and another one is solidification range.

As described in detail in experimental work, pore number and total pore length were calculated from T zones. The results of pore measurements are given in Figure 8. The maximum pore formation was found in A4 part of T zone in all alloys and all conditions. This zone has the hot spot. This location is also a point where turbulence occurs as seen in trace element results of MagmaSoft shown in Figure 9. Therefore, these results reflect how the pore formation occurs in test samples not just due to bifilms that are coming from the melt but due to the turbulence that generates new bifilms on the T-junction during filling of the mold. The stress and strain generated during solidification of these alloys

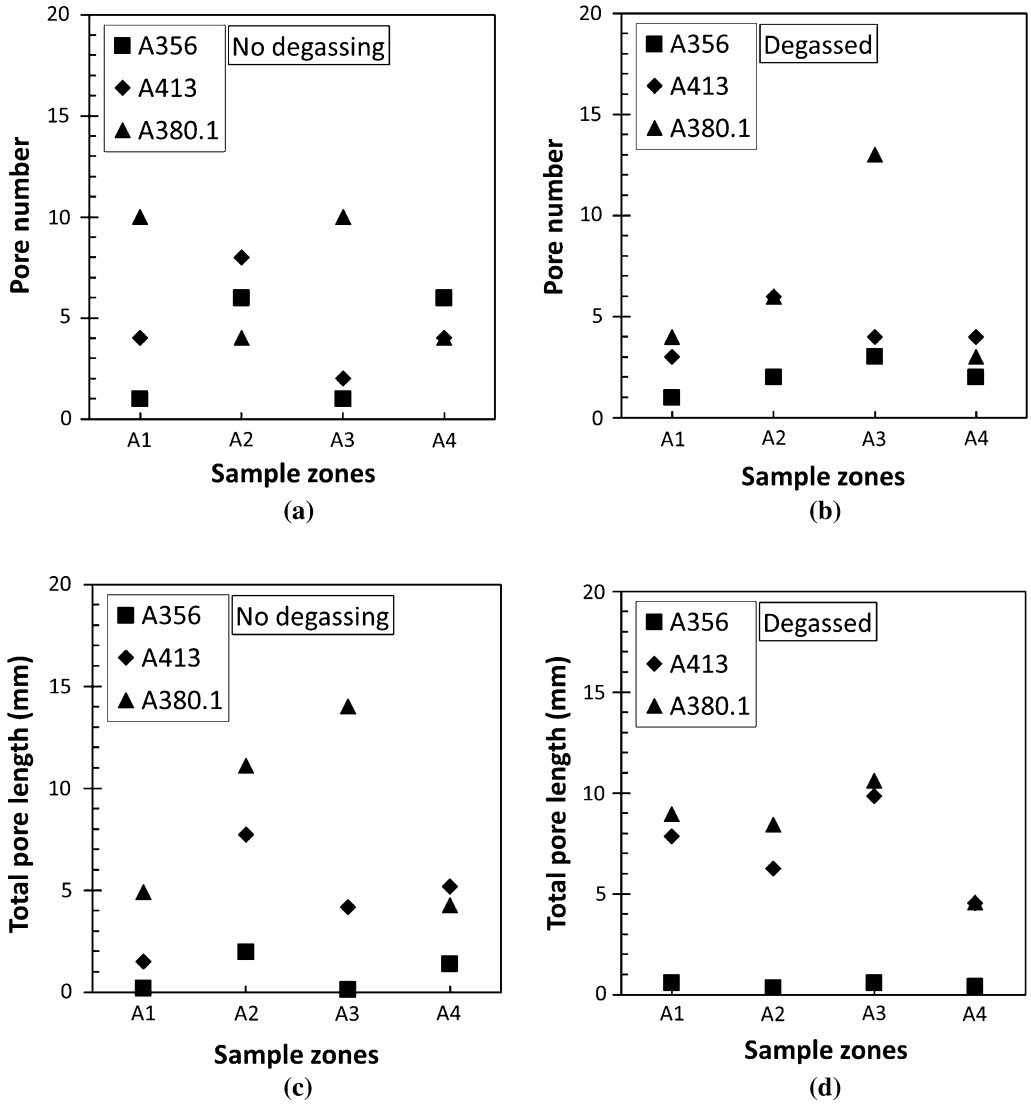

Fig. 13—(*a*) Pore numbers of cast parts from CRC mold for no degassing condition, (*b*) Pore numbers of cast parts from CRC mold for degassed condition, (*c*) total pore of cast parts from CRC mold for no degassing condition, and (*d*) total pore of cast parts from CRC mold for degassed condition.

have been simulated by Magma and the results are given in Figure 9(b). These stress and strain will aid in the unraveling of the bifilms.

With regard to pore analysis shown in Figure 8, it was found in the present study that the relationship between bifilms and hot tearing depends on distribution, number, size, and orientation of bifilms. For hot tearing defect to occur, four conditions given below should take place at the same time. This phenomenon is schematically given in Figure 10.

i. Distribution of bifilms should be intensified on A4 part in the hot spot.
ii. Number of bifilms should either be too high or too low. If it is the lowest, its size should be the greatest. If highest, it should be heterogeneously distributed between hot spot and T-junction regions.
iii. Size of bifilms should be large enough to trigger hot tearing
iv. The orientation of bifilms should be vertical to the direction of shrinkage in order to trigger hot tearing. If it is horizontal, hot tearing cannot occur.

It can be understood that orientation of bifilms is the most important factor to hot tearing formation (Figure 10). An example of actual cast parts is given in Figure 11. When there are too many bifilms in T zone, two different possibilities are accounted for. If A4 part of T zone has bifilms more than A2 part of T zone, hot tearing can occur. However, if A4 and A2 parts of T zone have almost the same amount of bifilms, hot tearing cannot occur, because the number of bifilms that causes porosity will balance stress distribution of solidification (that is the liquid/solid contraction). In this case, stress that is enough to tear alloy cannot take place. On the other hand, bifilms might be accumulated on A2 parts of T zone and so, the hot tearing cannot occur because of the insufficient number of bifilms on

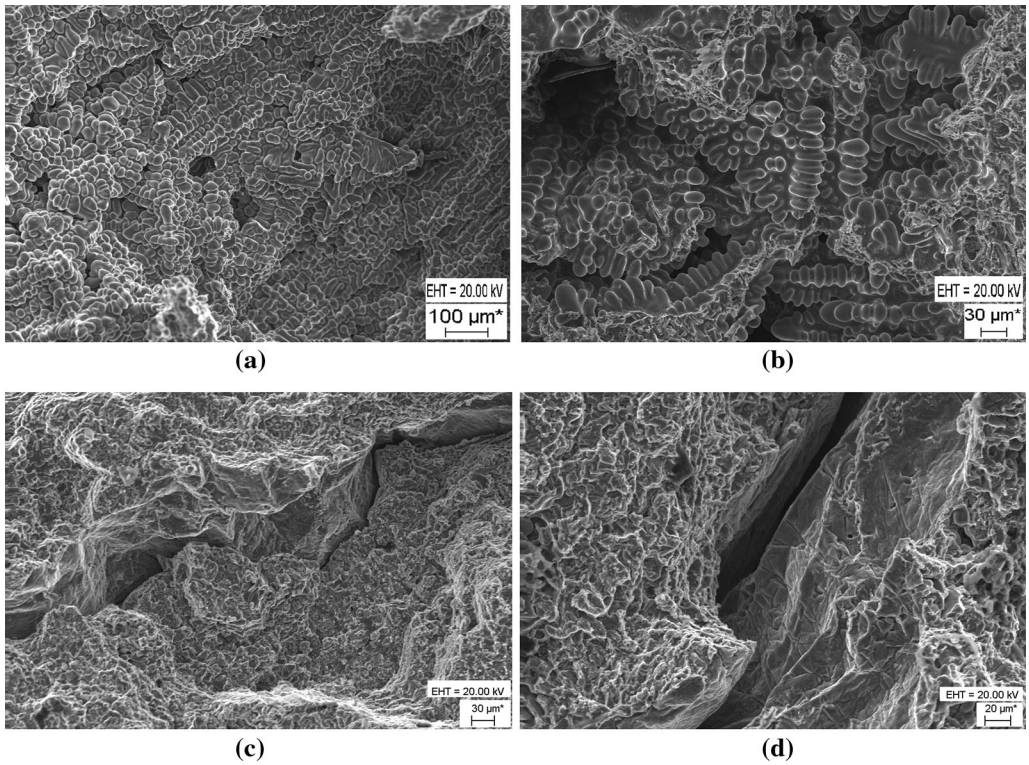

Fig. 14—SEM images for pore formation (*a*) A356 and (*b*) A380.1 alloys and for hot torn region (*c*, *d*) A380.1 alloy.

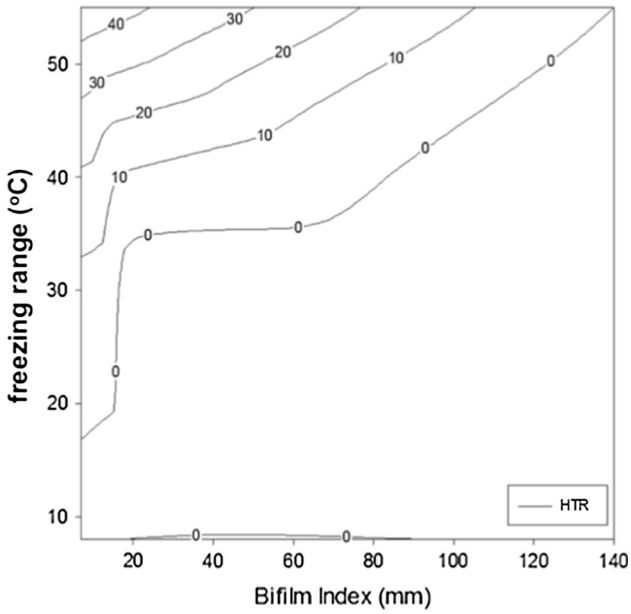

Fig. 15—Effect of freezing range and bifilm index on hot tearing.

A4. The last and the most important factor is the existence of large and vertically located bifilms along the hot spot region. If bifilms are large in size and few but vertical to the stress direction of shrinkage, hot tearing can occur easily. However, if they exist in large size and small amount but horizontal to the direction of shrinkage, it is very difficult to trigger hot tearing. On the other hand, surface sink is related with how many bifilms are present and how the feedability is effective. It can be realized that if there is enough number of opened bifilms in T zone, surface sink does not take place. However, if there is no or insufficient bifilms in T zone, surface sink can be seen on the surface. These comments about surface sink and pore formation were explained in detail in Reference 1. This work has also shown that this theoretical approach was experimentally proven.

CRC mold was also used in this study to investigate hot tearing formation. Cast parts of all alloys and all conditions for CRC mold are given in Figure 12. It was found that the results of CRC molds are quite similar to the results of T-shape mold. While there was no hot tearing in A356 and A413 alloy castings, there was various severity of hot tearing in A380.1 alloy castings. CRC mold has four different arms that have different lengths and spherical parts on the end of the arms. It was observed that surface sink occurred on the spherical parts in A356 and A380.1 alloys, but it did not occur in A413 alloy. This is due to the solidification morphology and solidification range. Measurements of pore formation from CRC mold were done and the results are given in Figure 13. As described in experimental details, spherical parts of the arms of CRC casting parts were cut vertically. One of these two parts was examined to calculate pore formation. It can be seen on the results that the minimum pore formation is in castings of A356 alloy, and the maximum pore formation is in castings of A380.1 alloy. An evidence for this role is shown in the SEM images in Figures 14(a) and (b). Oxides are clearly seen on the cross section of the hot torn parts in Figures 14(c) and (d). A356 has lower solidification

range than A380.1 alloy and columnar morphology. During the solidification, bifilms cannot be opened between the dendrite arms. However, A380.1 alloy has a high solidification range and two different eutectic morphology form in the microstructure. The structure of A380.1 alloy on the SEM image is more equiaxed and smaller than A356 alloy. During the solidification, the last region of liquid to solidify will aid in the unraveling of bifilms. Opened bifilms are the most dangerous defects for not only hot tearing but also several other properties of a cast part.

It is important to note that for the first time in literature, the concept of melt quality was introduced for hot tearing phenomena in cast Al-Si alloys. It was found that there is a strong relationship among freezing (solidification) range, bifilm index, and hot tearing susceptibility. The result of this relationship is shown in Figure 15. It shows that hot tearing formation depends on the freezing range and bifilm index. Hot tearing can occur at larger freezing range depending on the bifilm index value. With increased bifilm index (*i.e.*, low-quality melt), hot tearing decreases regardless of high freezing range. The extrapolation of results shows that (Figure 15), freezing ranges above 55 °C and bifilm index above 120 mm result in no hot tear. On the other hand, when bifilm index is between 40 and 100 mm, the hot tearing tendency might be decreased due to the distribution and orientation of bifilms. A single and large bifilm that is located perpendicularly along the hot spot stress direction will result in hot tearing, otherwise, bifilm will form porosity to compensate contraction.

IV. CONCLUSIONS

Bifilms are defects that are formed in the liquid state mainly due to the folding of surface oxide with turbulence. The oxide structure and severity of turbulence affect the length and characteristic of bifilm directly. In light of these explanations:

1. Hot tearing defect has not been seen in all alloys, because, distributions of solidification morphology and bifilms that form porosity are quite scattered. Once these bifilms are quantified, *i.e.*, RPT, their behavior and potential effects on the solidified alloy can be predicted.
2. Hot tearing does not occur under all casting conditions because size and distribution of bifilms that form porosity can be different in each casting depending on the bifilm size and content.
3. Hot tearing occurs randomly and indiscriminately because bifilms that form porosity are random and indiscriminate. If these bifilms are concentrated on hot spot area and are large in size, they can lead to hot tearing.
4. As the freezing range of the alloy is decreased, hot tearing tendency decreases. However, depending on the bifilm index, as it is increased, hot tearing is not observed even in long freezing range alloy because bifilms form porosity to compensate solidification contraction.

ACKNOWLEDGMENTS

Special thanks to Murat Akcin from MagmaSoft, Istanbul, Turkey for the simulations. This work has been supported by the Scientific Research Projects Coordination Unit of Selcuk University (Project Number: 13101026). Muhammet Uludağ was a Ph.D. student at Selcuk University, during the publication process, and he started working at Bursa Technical University. Author would like to thank to TUBITAK (Turkey) for its support.

REFERENCES

1. J. Campbell: *Complete Casting Handbook: Metal Casting Processes, Metallurgy*, Techniques and Design. Butterworth-Heinemann, Oxford, 2015.
2. D. Eskin and L. Katgerman: *Metall. Mater. Trans. A*, 2007, vol. 38A, pp. 1511–19.
3. C.H. Cáceres and B.I. Selling: *Mater. Sci. Eng., A*, 1996, vol. 220 (1–2), pp. 109–16.
4. T. Clyne, M. Wolf, and W. Kurz: *Metall. Trans. B*, 1982, vol. 13B, pp. 259–66.
5. M. M'Hamdi, A. Mo, and H.G. Fjær: *Metall. Mater. Trans. A*, 2006, vol. 37A, pp. 3069–83.
6. M. Rappaz, J.M. Drezet, and M. Gremaud: *Metall. Mater. Trans. A*, 1999, vol. 30A, pp. 449–55.
7. J. Spittle and A. Cushway: *Met. Technol.*, 1983, vol. 10 (1), pp. 6–13.
8. M. M'Hamdi, A. Mo, and C.L. Martin: *Metall. Mater. Trans. A*, 2002, vol. 33A, pp. 2081–93.
9. J. Campbell: *Castings: The New Metallurgy of Cast Metals*, Butterworth Heinemann, Oxford, 2003.
10. D.G. Eskin, Suyitno, and L. Katgerman: *Prog. Mater. Sci.*, 2004, vol. 49(5), pp. 629–711.
11. J. Verö: *Met. Ind.*, 1936, vol. 48, pp. 431–94.
12. W.I. Pumphrey and P.H. Jennings: *J. Inst. Metals*, 1948, vol. 75, pp. 235–56.
13. M.O. Pekguleryuz, S. Lin, E. Ozbakir, D. Temur, and C. Aliravci: *Int. J. Cast Met. Res.*, 2010, vol. 23 (5), pp. 310–20.
14. M. Pokorny, C. Monroe, C. Beckermann, L. Bichler, and C. Ravindran: *Int. J. Metalcast.*, 2008, vol. 2 (4), pp. 41–53.
15. L. Bichler, C. Ravindran, and D. Sediako: *Can. J. Phys.*, 2010, vol. 88 (10), pp. 715–21.
16. L. Bichler and C. Ravindran: *Mater. Des.*, 2010, vol. 31 (Supplement 1), pp. 17–23.
17. M.R.N. Esfahani and B. Niroumand: *Mater. Charact.*, 2010, vol. 61 (3), pp. 318–24.
18. F. D'Elia, C. Ravindran, and D. Sediako: *Can. Metall. Q.*, 2014, vol. 53 (2), pp. 151–59.
19. G. Cao and S. Kou: *Metall. Mater. Trans. A*, 2006, vol. 37A, pp. 3647–63.
20. S. Lin, C. Aliravci, and M.O. Pekguleryuz: *Metall. Mater. Trans. A*, 2007, vol. 38A, pp. 1056–68.
21. M.O. Pekguleryuz and P. Vermette: *Int. J. Cast Met. Res.*, 2009, vol. 22 (5), pp. 357–66.
22. H. Kamguo Kamga, D. Larouche, M. Bournane, and A. Rahem: *Mater. Sci. Eng., A*, 2010, vol. 527 (27–28), pp. 7413–23.
23. L. Katgerman: *JOM*, 1982, vol. 34 (2), pp. 46–49.
24. S. Li, K. Sadayappan, and D. Apelian: *Int. J. Cast Met. Res.*, 2011, vol. 24 (2), pp. 88–95.
25. S. Li, D. Apelian, and K. Sadayappan: *Int. J. Metalcast.*, 2012, vol. 6 (3), pp. 51–58.
26. S. Li, K. Sadayappan, and D. Apelian: *Metall. Mater. Trans. B*, 2013, vol. 44B, pp. 614–23.
27. A.K. Dahle, Y.C. Lee, M.D. Nave, P.L. Schaffer, and D.H. StJohn: *J. Light Met.*, 2001, vol. 1 (1), pp. 61–72.
28. C. Dickhaus, L. Ohm, and S. Engler: *AFS Trans.*, 1994, vol. 101, pp. 677–84.

29. D. Lahaie and M. Bouchard: *Metall. Mater. Trans. B*, 2001, vol. 32B, pp. 697–705.
30. J. Langlais and J.E. Gruzleski, in *Aluminium Alloys: Their Physical and Mechanical Properties, Pts 1-3*, E.A. Starke, T.H. Sanders, and W.A. Cassada, eds., Trans Tech Publications Ltd, Stafa-Zurich, 2000, pp. 167–72.
31. I. Novikov: *Goryachelomkost'tsvetnyh metallov i splavov*, Nauka, Novosibirsk, 1966, p. 299.
32. W. Suyitno Kool and L. Katgerman: *Mater. Sci. Forum*, 2002, vol. 179, pp. 396–402.
33. J. Williams and A. Singer: *J. Inst. Met.*, 1968, vol. 96, pp. 5–12.
34. B. Magnin, L. Maenner, L. Katgerman, and S. Engler: *Mater. Sci. Forum*, 1996, vols. 217–222, pp. 1209–14.
35. L. Zhao, N. Baoyin Wang, V. Sahajwalla, and R. Pehlke: *Int. J. Cast Met. Res.*, 2000, vol. 13 (3), pp. 167–74.
36. M. Braccini, C. Martin, M. Suery, and Y. Bréchet: *MCWASP IX*. Shaker Verlag, Aachen, 2000.
37. N.N. Prokhorov: *Russ. Cast. Prod.*, 1962, vol. 2, pp. 172–77.
38. T. Clyne and G. Davies: *Br. Foundrym.*, 1975, vol. 68, pp. 238–44.
39. U. Feurer: *Quality Control of Engineering Alloys and the Role of Metals Science*, Delft University of Technology, Delft, 1977, pp. 131–45.
40. D. Dispinar, S. Akhtar, A. Nordmark, M. Di Sabatino, and L. Arnberg: *Mater. Sci. Eng., A*, 2010, vol. 527 (16–17), pp. 3719–25.
41. G.E. Bozchaloei, N. Varahram, P. Davami, and S.K. Kim: *Mater. Sci. Eng., A*, 2012, vol. 548, pp. 99–105.
42. X. Cao, W. Wallace, J.-P. Immarigeon, and C. Poon: *Mater. Manuf. Process.*, 2003, vol. 18 (1), pp. 23–49.
43. A.K. Dey, P. Poddar, K.K. Singh, and K.L. Sahoo: *Mater. Sci. Eng., A*, 2006, vols. 435–436, pp. 521–29.
44. M. Tiryakioglu, J. Campbell, and N.D. Alexopoulos: *Metall. Mater. Trans. A*, 2009, vol. 40A, pp. 1000–07.
45. D. Dispinar and J. Campbell: *Int. J. Cast Met. Res.*, 2004, vol. 17 (5), pp. 280–86.
46. D. Dispinar and J. Campbell: *Int. J. Cast Met. Res.*, 2004, vol. 17 (5), pp. 287–94.
47. D. Dispinar and J. Campbell: *Int. J. Cast Met. Res.*, 2006, vol. 19 (1), pp. 5–17.
48. D. Dispinar and J. Campbell: *J. Mater. Process. Technol.*, 2007, vol. 182 (1–3), pp. 405–10.
49. D. Dispinar and J. Campbell: *Mater. Sci. Eng., A*, 2011, vol. 528 (10–11), pp. 3860–65.
50. D. Dispinar, A. Nordmark, J. Voje, and L. Arnberg: in *138th TMS Annual Meeting, Shape Casting: 3rd International Symposium*, San Francisco, California, USA, February 2009.
51. D. Dispinar and J. Campbell: in *Shape Casting: 5th International Symposium 2014*, Springer, Cham.
52. H. Bagherpour-Torghabeh, R. Raiszadeh, and H. Doostmohammadi: *Metall. Mater. Trans. B*, 2017, vol. 48 (6), pp. 3174–84.
53. H. Bartar Esfahani, R. Raiszadeh, and H. Doostmohammadi: *Int. J. Cast Met. Res.*, 2017, vol. 30 (2), pp. 87–95.
54. P. Davami, S. Kim, and M. Tiryakioğlu: *Mater. Sci. Eng., A*, 2013, vol. 579, pp. 64–70.
55. B. Farhoodi, R. Raiszadeh, and M.-H. Ghanaatian: *J. Mater. Sci. Technol.*, 2014, vol. 30 (2), pp. 154–62.
56. W. Li, J. Zhou, B. Ma, J. Wang, J. Wu, and Y. Yang: *Metall. Mater. Trans. B*, 2017, vol. 48B, pp. 2334–42.
57. B. Mirzaei, S. Akhtar, and R.E. Aune: in *IEEE 2013 International Conference on Aerospace Science & Engineering (ICASE)*, 2013.
58. M. Mostafaei, M. Ghobadi, M. Uludağ, and M. Tiryakioğlu: *Metall. Mater. Trans. B*, 2016, vol. 47B, pp. 3469–75.
59. G. Timelli and D. Caliari: *Mater. Sci. Forum.*, 2017, vols. 773–774, pp. 462–68.
60. M. Tiryakioğlu, P. Davami, S.-K. Kim, Y.O. Yoon, G.-Y. Yeom, and N.-S. Kim: *Mater. Sci. Eng., A*, 2014, vol. 605, pp. 203–09.
61. M. Uludağ, R. Çetin, D. Dispinar, and M. Tiryakioğlu: *Metals*, 2017, vol. 7 (5), p. 157.
62. J. Campbell: *Castings Practice—The 10 Rules for Casting*, Elsevier/Elsevier Butterworth-Heinemann, Oxford, Oxford, 2004.